Transient Analysis of Microstrip Line on Anisotropic Substrate in Three-Dimensional Space

SHOICHI KOIKE, MEMBER, IEEE, NORINOBU YOSHIDA, MEMBER, IEEE, AND ICHIRO FUKAI, MEMBER IEEE

Abstract —**The recent development of MIC demands considerable attention to the anisotropy of substrates such as sapphire in order to both utilize its characteristics and eliminate its undesirable features. Anisotropic materials usually have a three-dimensional structure, and yield complex characteristics in wave propagation. Hence the analysis requires an exact three-dimensional treatment using all electromagnetic field components. Also, progress in high-speed pulse techniques demands analysis in the time domain.**

This paper describes how the anisotropy, with the permittivity tensor involving off-diagonal elements, may be generally formulated by Bergeron's method. The formulation is discussed in the case of the propagation characteristics for single and parallel strip lines on a sapphire substrate with tilted optical axis. Furthermore, to show the distinctive influence of anisotropy on the coupling property between lines, a parallel-line-type directional coupler on such a substrate is analyzed.

I. Introduction

THE RECENT DEVELOPMENT of MIC demands considerable attention to the anisotropy of substrates, such as sapphire, regarding both utilization of its characteristics and elimination of its undesirable effects. The analysis of an electromagnetic field in a region including such an anisotropic medium is necessary not only for a rigorous treatment of medium characteristics, but also for gaining information for improving the characteristics of devices [1]–[3]. The structure of an MIC, consisting of a strip conductor, a ground plane, and an inhomogeneous substrate, imposes restrictions on the range of variation of the characteristic impedance and propagation constant or coupling property between lines. The anisotropic medium would be utilized to ameliorate this disadvantage of the microstrip structure [4], [5]. Also, in recent high-speed pulse techniques, dispersive characteristics caused by a small anisotropy of the substrate become a subject of concern.

Anisotropic substrates demand an exact three-dimensional treatment using all electromagnetic field components. Furthermore, analysis of the propagation of a pulse wave requires computation in the time domain. Transient analysis of the electromagnetic field is useful not only in clarifying the field response but also in providing information on the mechanism by which the distribution of the electromagnetic field in the stationary state is brought about. As a time-domain vector analysis method for a three-dimensional electromagnetic field, the FD–TD method proposed by Yee [6], [7] and the TLM method by Johns [8], [9] are used. For the problems involving anisotropic medium, the latter method has already been adopted [10], [11]. But for both methods it is difficult to formulate cases having tilted optical axes expressed by permittivity or permeability tensor with off-diagonal elements. We have proposed a method using an equivalent circuit of the electromagnetic field formulated by Bergeron's method, referred to here as the present method [12]–[15]. In this, the basic concept of the treatment of the condition of the medium is expressed by lumped elements at each node in the equivalent circuit. This treatment can be realized by Bergeron's formulation with the use of the voltage variable and two current variables for two different directions at each node. This feature is extended to the anisotropic medium by use of the mutual coupling between currents relating to the off-diagonal components in the permittivity or permeability tensor [16].

In this paper the treatment of anisotropy by Bergeron's method is extended to the three-dimensional vector analysis in the time domain for dielectric materials with a tensor involving off-diagonal elements. Initially it is proved that the equivalent circuit with the mutual coupling represents anisotropy with off-diagonal elements in the permittivity tensor. Next, the formulation is discussed by estimating the impedance and effective dielectric constants for single and parallel strip lines on a sapphire substrate as a function of a tilted angle. Lastly, to show the effect of anisotropy on the coupling property between two lines, a parallel-line directional coupler on such a substrate is analyzed, and its characteristics are presented.

II. Treatment of Anisotropic Medium

In this paper, we treat the anisotropy [16], [17] of the dielectric constant caused by tilt of an optical axis. In the present method the medium conditions are expressed by lumped elements at appropriate nodes. The off-diagonal elements in the permittivity tensor of the dielectric substrate demand the coupling of electric fields between different directions. The lumped circuit for those should be

Manuscript received March 5, 1987; revised July 30, 1987.

S. Koike is with the Space and Radio Division of Fujitsu Laboratories Ltd., Kawasaki 211, Japan.

N. Yoshida and I. Fukai are with the Department of Electrical Engineering, Hokkaido University, Sapporo, 060 Japan.

IEEE Log Number 8717590.

0018-9480/88/0100-0034$01.00 ©1988 IEEE

TABLE I
CORRESPONDENCE BETWEEN THE FIELD VARIABLES IN MAXWELL'S EQUATION AND THE EQUIVALENT CIRCUIT

	Electric node			Magnetic node	
	Maxwell's equations	Variables		Maxwell's equations	Variables
A k	$\frac{\partial Hx}{\partial z}-\frac{\partial Hz}{\partial x}=\varepsilon_0\frac{\partial Ey}{\partial t}$	$Vy\equiv Ey$	F k	$\frac{\partial Ex}{\partial z}-\frac{\partial Ez}{\partial x}=-\mu_0\frac{\partial Hy}{\partial t}$	$V\dot{y}^*\equiv Hy$
	$-\frac{\partial Ey}{\partial z}=-\mu_0\frac{\partial Hx}{\partial t}$	$Iz\equiv -Hx$		$-\frac{\partial Hy}{\partial z}=\varepsilon_0\frac{\partial Ex}{\partial t}$	$I\dot{z}^*\equiv Ex$
	$\frac{\partial Ey}{\partial x}=-\mu_0\frac{\partial Hz}{\partial t}$	$Ix\equiv Hz$		$\frac{\partial Hy}{\partial x}=\varepsilon_0\frac{\partial Ez}{\partial t}$	$I\dot{x}^*\equiv -Ez$
D k	$\frac{\partial Hz}{\partial y}-\frac{\partial Hy}{\partial z}=\varepsilon_0\frac{\partial Ex}{\partial t}$	$Vx\equiv Ex$	B k	$\frac{\partial Ey}{\partial x}-\frac{\partial Ex}{\partial y}=-\mu_0\frac{\partial Hz}{\partial t}$	$V\dot{z}^*\equiv Hz$
	$\frac{\partial Ex}{\partial z}=-\mu_0\frac{\partial Hy}{\partial t}$	$Iz\equiv Hy$		$\frac{\partial Hz}{\partial y}=\varepsilon_0\frac{\partial Ex}{\partial t}$	$I\dot{y}^*\equiv -Ex$
	$-\frac{\partial Ex}{\partial y}=-\mu_0\frac{\partial Hz}{\partial t}$	$Iy\equiv -Hz$		$-\frac{\partial Hz}{\partial x}=\varepsilon_0\frac{\partial Ey}{\partial t}$	$I\dot{x}^*\equiv Ey$
E k	$\frac{\partial Hy}{\partial x}-\frac{\partial Hx}{\partial y}=\varepsilon_0\frac{\partial Ez}{\partial t}$	$Vz\equiv -Ez$	C k	$\frac{\partial Ez}{\partial y}-\frac{\partial Ey}{\partial z}=-\mu_0\frac{\partial Hx}{\partial t}$	$V\dot{x}^*\equiv -Hx$
	$\frac{\partial Ez}{\partial y}=-\mu_0\frac{\partial Hx}{\partial t}$	$Iy\equiv -Hx$		$\frac{\partial Hx}{\partial z}=\varepsilon_0\frac{\partial Ey}{\partial t}$	$I\dot{z}^*\equiv Ey$
	$-\frac{\partial Ez}{\partial x}=-\mu_0\frac{\partial Hy}{\partial t}$	$Ix\equiv Hy$		$-\frac{\partial Hx}{\partial y}=\varepsilon_0\frac{\partial Ez}{\partial t}$	$I\dot{y}^*\equiv -Ez$
dielectric constant	$C_0=\varepsilon_0/2$		dielectric constant	$L_0^*=\varepsilon_0/2$	
permeability	$L_0=\mu_0/2$		permeability	$C_0^*=\mu_0/2$	
polarization	$\Delta C=\varepsilon_0\chi e/2\cdot\Delta d$		magnetization	$\Delta C^*=\mu_0\chi m/2\cdot\Delta d$	
conductivity	$G=\sigma/2\cdot\Delta d$		magnetic current loss	$G^*=\sigma^*/2\cdot\Delta d$	
magnetization	$\Delta L=\mu_0\chi m/2\cdot\Delta d$		polarization	$\Delta L^*=\varepsilon_0\chi e/2\cdot\Delta d$	

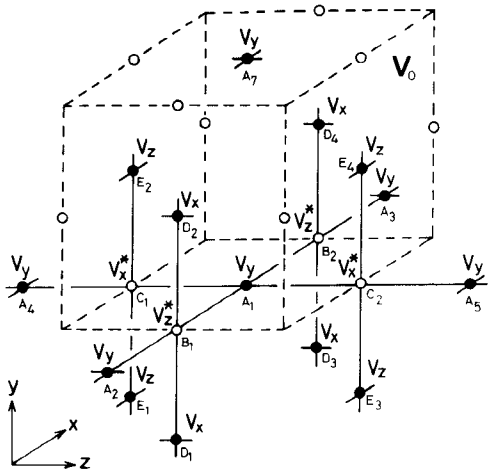

Fig. 1. Arrangement of nodes around A_1.

given at a node in which either of the coupled electric field components exists. Such a condition is satisfied at the magnetic node in which the electric fields correspond to the current variables. Therefore, given the duality of circuit variables, the diagonal and off-diagonal components of the dielectric constant are expressed by self-inductance and mutual inductance, respectively.

In this section we prove that the equivalent circuit consisting of inductance with mutual coupling at magnetic nodes represents the electromagnetic wave equation in the anisotropic dielectric medium. We assume coupling between the electric fields E_y and E_x, and use circuit variables as shown in Table I. Fig. 1 shows the arrangement of nodes around the A_1 node in which the voltage variable V_y corresponds to the electric field E_y. Fig. 2 shows details of nodes A, B, and C. At the B nodes, lumped inductances involving mutual coupling give the property of anisotropic dielectric constant. Central difference equations are derived at all nodes B_1, B_2, and C_1, C_2 that are adjacent to node A_1 as follows;

$$V_y(A_2)-V_y(A_1)=2\Delta x C_0^*\,\partial_t V_z^*(B_1) \quad (1a)$$

$$V_y(A_1)-V_y(A_3)=2\Delta x C_0^*\,\partial_t V_z^*(B_2) \quad (1b)$$

$$-\{V_x(D_1)-V_x(D_2)\}=2\Delta y C_0^*\,\partial_t V_z^*(B_1) \quad (1c)$$

$$-\{V_x(D_3)-V_x(D_4)\}=2\Delta y C_0^*\,\partial_t V_z^*(B_2) \quad (1d)$$

$$V_y(A_4)-V_y(A_1)=2\Delta z C_0^*\,\partial_t V_x^*(C_1) \quad (1e)$$

$$V_y(A_1)-V_y(A_5)=2\Delta z C_0^*\,\partial_t V_x^*(C_2) \quad (1f)$$

$$V_z(E_1)-V_z(E_2)=2\Delta y C_0^*\,\partial_t V_x^*(C_1) \quad (1g)$$

$$V_z(E_3)-V_z(E_4)=2\Delta y C_0^*\,\partial_t V_x^*(C_2) \quad (1h)$$

where Δx, Δy, and Δz are the lattice intervals in the x, y, and z directions, respectively, and are equal to the constant value Δd. C_0^* corresponds to the free-space permeability μ_0 shown in Table I, and ∂_t denotes $\partial/\partial t$ for simplicity. In the following equations, for simplicity ∂_x, ∂_y, and ∂_z also denote $\partial/\partial x$, $\partial/\partial y$, and $\partial/\partial z$, respec-

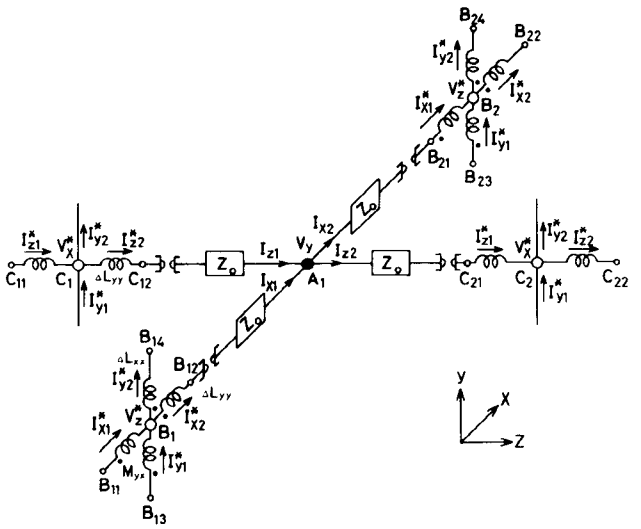

Fig. 2. Details of nodes A, B, and C.

tively. Negative signed braces in (1c) and (1d) are derived from the opposite sign in the corresponding variables between the B and D nodes.

Next, the voltages V_z^*, V_x^* at B_1, B_2 and C_1, C_2 are expressed by current components I_{z1}, I_{z2} and I_{x1}, I_{x2} at A_1, as shown in Fig. 2. The voltage at B_1 is expressed as follows by using $\partial_x V_z^* = -L_0^* \partial_t I_x^*$:

$$\begin{aligned} V_z^*(B_1) &= I_{x1}(A_1) - \Delta x \partial_x V_z^*(B_{12}) + \Delta V_z^*(B_{12}) \\ &= I_{x1}(A_1) + L_0^* \Delta x \partial_t I_{x2}^*(B_{12}) \\ &\quad + \Delta L_{yy}^* \Delta x \partial_t I_{x2}^*(B_{12}) \\ &\quad + M_{yx}^* \Delta y \partial_t \{ -I_y^*(B_{13}) - I_y^*(B_{14}) \} \end{aligned} \quad (2a)$$

where $V_z^*(B_{12})$ is the voltage drop at an inductance. At other nodes, the following relations are also formulated in the same manner.

$$\begin{aligned} V_z^*(B_2) &= I_{x2}(A_1) - L_0^* \Delta x \partial_t I_{x1}^*(B_{21}) \\ &\quad - \Delta L_{yy}^* \Delta x \partial_t I_{x1}^*(B_{21}) \\ &\quad - M_{yx}^* \Delta y \partial_t \{ -I_y^*(B_{23}) - I_y^*(B_{24}) \} \end{aligned} \quad (2b)$$

$$\begin{aligned} V_x^*(C_1) &= I_{z1}(A_1) + L_0^* \Delta z \partial_t I_{z2}^*(C_{12}) \\ &\quad + \Delta L_{yy}^* \Delta z \partial_t I_{z2}^*(C_{12}) \end{aligned} \quad (2c)$$

$$\begin{aligned} V_x^*(C_2) &= I_{z2}(A_1) - L_0^* \Delta z \partial_t I_{z1}^*(C_{21}) \\ &\quad - \Delta L_{yy}^* \Delta z \partial_t I_{z1}^*(C_{21}). \end{aligned} \quad (2d)$$

Substituting (2) into (1) gives

$$\begin{aligned} &V_y(A_2) - V_y(A_1) \\ &\quad = 2\Delta x C_0^* \partial_t I_{x1}(A_1) + 2\Delta x^2 C_0^* L_0^* \partial_t^2 I_{x2}^*(B_{12}) \\ &\qquad + 2\Delta x^2 \Delta L_{yy}^* C_0^* \partial_t^2 I_{x2}^*(B_{12}) \\ &\qquad + 2\Delta x \Delta y M_{yx}^* C_0^* \partial_t^2 \{ -I_y^*(B_{13}) - I_y^*(B_{14}) \} \end{aligned} \quad (3a)$$

$$\begin{aligned} &V_y(A_1) - V_y(A_3) \\ &\quad = 2\Delta x C_0^* \partial_t I_{x2}(A_1) - 2\Delta x^2 C_0^* L_0^* \partial_t^2 I_{x1}^*(B_{21}) \\ &\qquad - 2\Delta x^2 \Delta L_{yy}^* C_0^* \partial_t^2 I_{x1}^*(B_{21}) \\ &\qquad - 2\Delta x \Delta y M_{yx}^* C_0^* \partial_t^2 \{ -I_y^*(B_{23}) - I_y^*(B_{24}) \} \end{aligned} \quad (3b)$$

$$\begin{aligned} &-\{ V_x(D_1) - V_x(D_2) \} \\ &\quad = 2\Delta y C_0^* \partial_t I_{x1}(A_1) + 2\Delta y \Delta x C_0^* L_0^* \partial_t^2 I_{x2}^*(B_{12}) \\ &\qquad + 2\Delta y \Delta x \Delta L_{yy}^* C_0^* \partial_t^2 I_{x2}^*(B_{12}) \\ &\qquad + 2\Delta y^2 M_{yx}^* C_0^* \partial_t^2 \{ -I_y^*(B_{13}) - I_y^*(B_{14}) \} \end{aligned} \quad (3c)$$

$$\begin{aligned} &-\{ V_x(D_3) - V_x(D_4) \} \\ &\quad = 2\Delta y C_0^* \partial_t I_{x2}(A_1) - 2\Delta y \Delta x C_0^* L_0^* \partial_t^2 I_{x1}^*(B_{21}) \\ &\qquad - 2\Delta y \Delta x \Delta L_{yy}^* C_0^* \partial_t^2 I_{x1}^*(B_{21}) \\ &\qquad - 2\Delta y^2 M_{yx}^* C_0^* \partial_t^2 \{ -I_y^*(B_{23}) - I_y^*(B_{24}) \} \end{aligned} \quad (3d)$$

$$\begin{aligned} &V_y(A_4) - V_y(A_1) \\ &\quad = 2\Delta z C_0^* \partial_t I_{z1}(A_1) + 2\Delta z^2 C_0^* L_0^* \partial_t^2 I_{z2}^*(C_{12}) \\ &\qquad + 2\Delta z^2 \Delta L_{yy}^* C_0^* \partial_t^2 I_{z2}^*(C_{12}) \end{aligned} \quad (3e)$$

$$\begin{aligned} &V_y(A_1) - V_y(A_5) \\ &\quad = 2\Delta z C_0^* \partial_t I_{z2}(A_1) - 2\Delta z^2 C_0^* L_0^* \partial_t^2 I_{z1}^*(C_{21}) \\ &\qquad - 2\Delta z^2 \Delta L_{yy}^* C_0^* \partial_t^2 I_{z1}^*(C_{21}) \end{aligned} \quad (3f)$$

$$\begin{aligned} &V_z(E_1) - V_z(E_2) \\ &\quad = 2\Delta y C_0^* \partial_t I_{z1}(A_1) + 2\Delta y \Delta z C_0^* L_0^* \partial_t^2 I_{z2}^*(C_{12}) \\ &\qquad + 2\Delta y \Delta z \Delta L_{yy}^* C_0^* \partial_t^2 I_{z2}^*(C_{12}) \end{aligned} \quad (3g)$$

$$\begin{aligned} &V_z(E_3) - V_z(E_4) \\ &\quad = 2\Delta y C_0^* \partial_t I_{z2}(A_1) - 2\Delta y \Delta z C_0^* L_0^* \partial_t^2 I_{z1}^*(C_{21}) \\ &\qquad - 2\Delta y \Delta z \Delta L_{yy}^* C_0^* \partial_t^2 I_{z1}^*(C_{21}). \end{aligned} \quad (3h)$$

Assuming that $\Delta x = \Delta y = \Delta z = \Delta d$, to satisfy the continuity of currents I_{z1}, I_{z2}, I_{x1}, and I_{x2} at the A_1 node, which are included in the first term of the right side of each equation in (3), the operation (3a) − (3b) + (3c) − (3d) + (3e) − (3f) + (3g) − (3h) is performed to give

$$\begin{aligned} &\{ V_y(A_2) + V_y(A_3) - 2V_y(A_1) \} \\ &\quad + \{ V_y(A_4) + V_y(A_5) - 2V_y(A_1) \} \\ &\quad + \{ -V_y(D_1) + V_x(D_3) + V_z(E_1) - V_z(E_3) \} \\ &\quad + \{ -V_y(D_4) + V_x(D_2) + V_z(E_4) - V_z(E_2) \} \\ &\quad = 4\Delta d C_0^* \partial_t \{ I_{x1} - I_{x2} + I_{z1} - I_{z2} \}|_{A_1} \\ &\qquad + 4\Delta d^2 C_0^* L_0^* \partial_t^2 \{ I_{x2}^*(B_{12}) + I_{x1}^*(B_{21}) \\ &\qquad + I_{z2}^*(C_{12}) + I_{z1}^*(C_{21}) \} \\ &\qquad + 4\Delta d \Delta L_{yy}^* C_0^* \partial_t^2 \{ I_{x2}^*(B_{12}) + I_{x1}^*(B_{21}) \\ &\qquad + I_{z2}^*(C_{12}) + I_{z1}^*(C_{21}) \} \\ &\qquad + 4\Delta d^2 M_{yx}^* C_0^* \partial_t^2 \{ -I_y^*(B_{13}) - I_y^*(B_{14}) \\ &\qquad - I_y^*(B_{23}) - I_y^*(B_{24}) \}. \end{aligned} \quad (4)$$

The first term in the right hand side of (4) is eliminated by applying Kirchhoff's first law at the A_1 node. Dividing both sides by $4\Delta d^2$ and allowing Δd to approach zero, the left side converges to ∇^2 using the divergence theorem under a no-space-charge condition in volume V_0 in Fig. 2:

$$\text{left side of (4)} = \nabla^2 V_y|_{A_1}. \tag{5a}$$

Also, the right side is transformed as follows:

$$\begin{aligned}
&\text{right side of (4)}\\
&= 4C_0^*L_0^*\,\partial_t^2\{I_{x2}^*(B_{12}) + I_{x1}^*(B_{21})\\
&\quad + I_{z2}^*(C_{12}) + I_{z1}^*(C_{21})\}/4\\
&\quad + 4\Delta L_{yy}^* C_0^*\,\partial_t^2\{I_{x2}^*(B_{12}) + I_{x1}^*(B_{21})\\
&\quad + I_{z2}^*(C_{12}) + I_{z1}^*(C_{21})\}/4\\
&\quad + 4M_{yx}^*C_0^*\,\partial_t^2\{-I_y^*(B_{13}) - I_y^*(B_{14})\\
&\quad - I_y^*(B_{23}) - I_y^*(B_{24})\}/4\\
&= 4C_0^*\left(L_0^* + \Delta L_{yy}^*\right)\partial_t^2\\
&\quad \cdot\left\{\frac{I_{x2}^*(B_{12}) + I_{x1}^*(B_{21}) + I_{z2}^*(C_{12}) + I_{z1}^*(C_{21})}{4}\right\}\\
&\quad + 4C_0^*M_{yx}^*\,\partial_t^2\\
&\quad \cdot\left\{\frac{-I_y^*(B_{13}) - I_y^*(B_{14}) - I_y^*(B_{23}) - I_y^*(B_{24})}{4}\right\}.
\end{aligned} \tag{5b}$$

Here as Δd approaches zero all variables approach the values at the center node A_1:

$$\begin{aligned}
(5b) &= 4C_0^*L^*\left.\frac{\partial^2 V_y}{\partial t^2}\right|_{A_1}\\
&\quad + 4C_0^*M_{yx}^*\cdot\left.\frac{\partial^2(-I_y^*)}{\partial t^2}\right|_{\text{between } B_1 \text{ and } B_2, \text{ namely } A_1}.
\end{aligned} \tag{6}$$

For generality we omit the position notation A_1. As a result, (5a) and (6) yield the wave equation,

$$\nabla^2 V_y = 4C_0^*L^*\frac{\partial^2 V_y}{\partial t^2} + 4C_0^*M_{yx}^*\frac{\partial^2(-I_y^*)}{\partial t^2}. \tag{7}$$

From correspondence of variables, $V_y|_A = E_y$, $-I_y^*|_B = E_x$, $L_0^* = \varepsilon_0/2$, $C_0^* = \mu_0/2$, $L^* = L_0^* + \Delta L_{yy}^* = \varepsilon_0(1+\chi_{yy})/2 = \varepsilon_0\varepsilon_{yy}/2$, and $M_{yx}^* = \varepsilon_0\varepsilon_{yx}/2$ are derived. Therefore, (7) represents the following electromagnetic wave equation in the anisotropic medium:

$$\nabla^2 E_y = \varepsilon_0\varepsilon_{yy}\mu_0\frac{\partial^2 E_y}{\partial t^2} + \varepsilon_0\varepsilon_{yx}\mu_0\frac{\partial^2 E_x}{\partial t^2}. \tag{8}$$

At other nodes in which the coupling between different field components occurs, the same fomulations may be derived.

We omit the description of Bergeron's formulation because the approximation of inductance and mutual coupling in the time domain by the trapezoidal rule is similar to that for capacitance [12].

III. Analytical Results and Discussion

The anisotropy used in this analysis is represented by the following dielectric tensor:

$$\varepsilon = \varepsilon_0\begin{bmatrix}\varepsilon_\xi & 0 & 0\\ 0 & \varepsilon_\eta & 0\\ 0 & 0 & \varepsilon_z\end{bmatrix}. \tag{9}$$

In (9), ε_ξ and ε_η are the principal optical axes of the relative dielectric constants of the substrate. The $\xi\eta$ coordinate system may be tilted with respect to the xy coordinate system by an angle θ, as shown in Fig. 3. Using the coordinate transformation, the permittivity tensor ε in the xyz coordinate system is given by

$$\varepsilon = \varepsilon_0\begin{bmatrix}\varepsilon_{xx} & \varepsilon_{yx} & 0\\ \varepsilon_{yx} & \varepsilon_{yy} & 0\\ 0 & 0 & \varepsilon_z\end{bmatrix} \tag{10}$$

where

$$\varepsilon_{xx} = \varepsilon_\xi\cos^2\theta + \varepsilon_\eta\sin^2\theta \tag{11a}$$

$$\varepsilon_{yx} = (\varepsilon_\eta - \varepsilon_\xi)\sin\theta\cos\theta \tag{11b}$$

$$\varepsilon_{yy} = \varepsilon_\xi\sin^2\theta + \varepsilon_\eta\cos^2\theta. \tag{11c}$$

A. Characteristic Impedance and Effective Dielectric Constant

In order to verify the validity of the treatment of anisotropy in the present method, we calculated the characteristic impedance Z and effective dielectric constant ε_{eff} of a microstrip line and parallel strip lines on the anisotropic substrate as a function of tilt angles. The relationship between the tilted principal axes $\varepsilon_\xi, \varepsilon_\eta$ of dielectric constant and coordinate axes x, y is shown in Fig. 3. Fig. 3(a) and (b) shows the cross sections of microstrip line and parallel microstrip lines, respectively. The strip and ground conductor are assumed to have infinite conductivity. The dimensions of Fig. 3(a) are $W/H = 0.5$, $a/H = 10$, and $b/H = 3.5$, and of Fig. 3(b) are $W/H = 1.0$, $S/H = 0.5$, $a/H = 10$, and $b/H = 3.5$. We consider sapphire as the anisotropic substrate, and assume that ε_ξ, ε_η and ε_z are 9.4, 11.6, and 9.4, respectively. In this analysis, the height of the substrate $H = 4\Delta d$, and one period of the applied sinusoidal wave is $T = 213\Delta t$, where Δt is the time interval between iterations. When $1\Delta d$ is assumed to be 0.15 mm, the frequency is $f = 18.78$ GHz, and the height of the dielectric substrate becomes $H = 0.6$ mm. If all space is filled with dielectric ($\varepsilon_r = 11.6$), the wavelength λ_g becomes $31.27\Delta d$. It is generally known that the number of divisions of the period and the wavelength should be more than ten in the difference formulation. Therefore, the numbers of divisions for the period and wavelength in this analysis are sufficient for good resolution in time and space. In this condition, since the dimension of each part of the transmission line structure is very small compared with the guide wavelength λ_g, a quasi-static field condition giving TEM wave propagation may be assumed.

The characteristic quantities are evaluated as follows in this analysis. The definition of characteristic impedance of

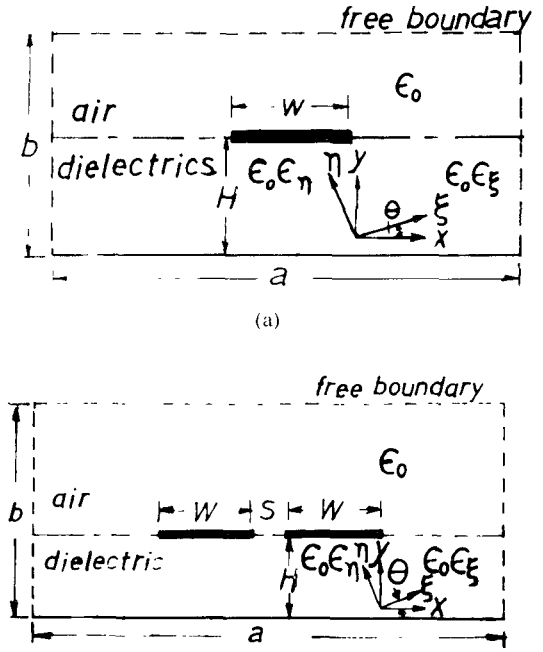

Fig. 3. $\xi\eta$ system coordinate tilted with respect to xy coordinate system by an angle θ. (a) Cross section of microstrip line. (b) Cross section of parallel microstrip lines.

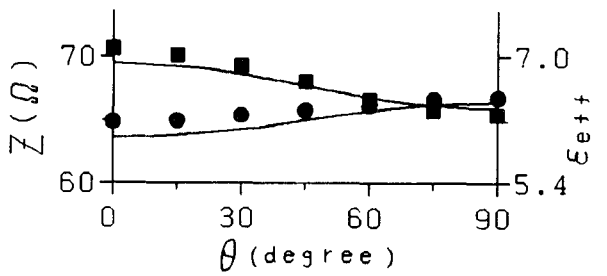

Fig 4 Characteristic impedance and effective dielectric constant of the microstrip line as a function of tilt angle.

microstrip is

$$Z = 2P_z/I_0^2 \tag{12}$$

and of two parallel strip lines is

$$Z = P_z/I_0^2 \tag{13}$$

where P_z is the time average of the Poynting vector propagating in the z direction, and I_0 is the magnitude of the conduction current in one strip line. The Poynting vector propagating in the z direction is given by $E_x \times H_y$ and $E_y \times (-H_x)$. Hence P_z is found by integrating these quantities in the xy cross section and by averaging the result over one period. I_0 can be found by a line integral of the magnetic field along the integration path around the strip conductor. The effective dielectric constants may be found from the ratio of the free-space wavelength λ_0 to the guide wavelength λ_g. Fig. 4 shows computed results of the characteristic impedance and effective dielectric constant of microstrip line as a function of tilt angle. The symbols ■,● present characteristic impedance and effective dielectric constant by the present method, and the curves show analytical results [1]. In [1] the analyzed subject is shielded, but the position of the shield is very far from the strip line, so our results, agree well with the analytical ones. The principal electric field of the propagating wave in the single stripline is E_y. When $\theta = 0°$, the η axis coincides with the y axis, so ε_{eff} is affected mainly by ε_η. ε_{eff} decreases and Z increases as ε_ξ becomes more effective through an increase of θ by rotating the anisotropic principal axis. Fig. 5 shows computed results of the even- and odd-mode characteristic impedances Z_{0e}, Z_{0o} and the effective dielectric constants $\varepsilon_{eff,even}$ and $\varepsilon_{eff,odd}$ of parallel microstrip lines as a function of tilt angle. The symbol ● denotes the results by the present method, and the curves indicate the analytical results [1]. In the case of the even mode, the fundamental electric field of the propagating wave is E_y, so that $\varepsilon_{eff,even}$ decreases and Z_{0e} increases with θ increasing, as in the case of the single strip line shown in Fig. 4. On the other hand, for the case of the odd mode, between the strip lines there exists a notable x-directed component of the electric field in the propagating wave; hence the variation of Z_{0o} and $\varepsilon_{eff,odd}$ with increasing θ is not so evident as in the case of the even mode. But the variation of each curve with θ has the same tendency as that of the even mode. Thus the analytical curves and our results agree within a few percent, and the validity of treating anisotropy by the present method is confirmed.

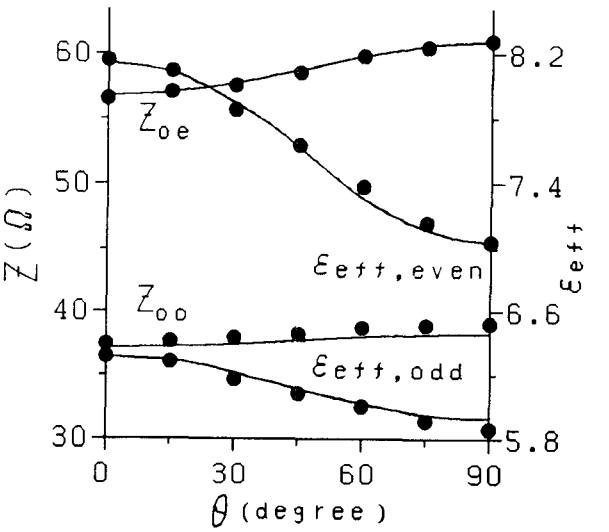

Fig. 5. Even- and odd-mode characteristic impedance and effective dielectric constant of the parallel microstrip lines as a function of tilt angle

B. Time Dependence with θ Variation of Propagation of Pulse Waves

To demonstrate the typical variation of propagation characteristics as a function of the tilt angle θ, we present the time variation of the propagation of the pulse wave for single strip line. The values of the relative dielectric constants in the principal axes of the anisotropic substrate, ε_ξ, ε_η and ε_z, are chosen to be 1.75, 2.5, and 1.75, respectively. The large ratio of ε_ξ to ε_η gives a distinct change in the

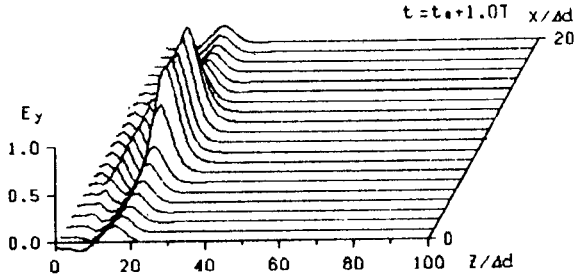

(a)

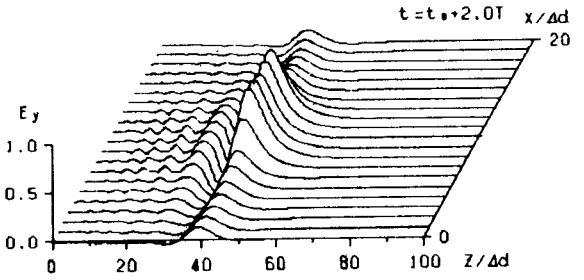

(b)

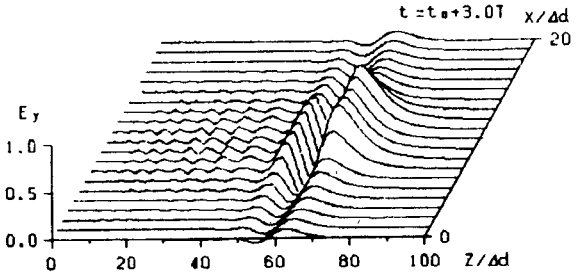

(c)

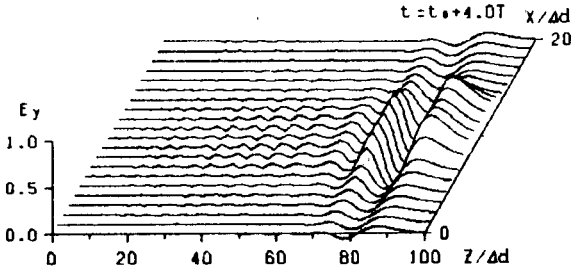

(d)

Fig 6 Time variation of pulse wave in microstrip line at $\theta = 0°$.

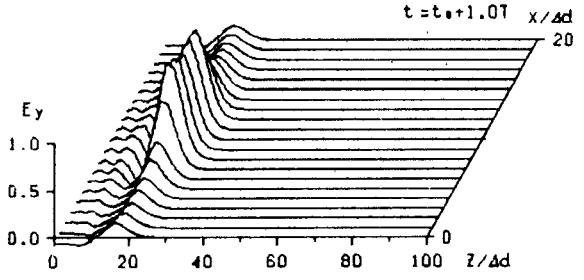

(a)

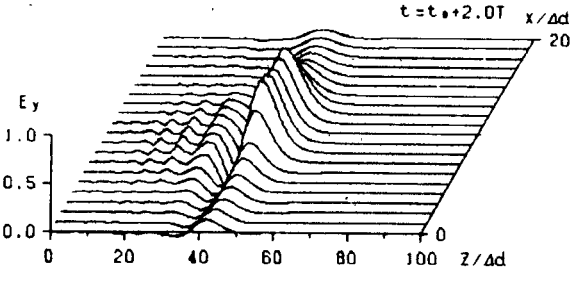

(b)

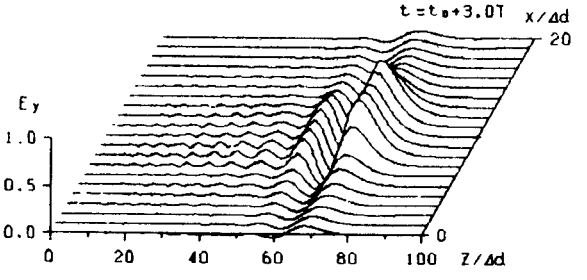

(c)

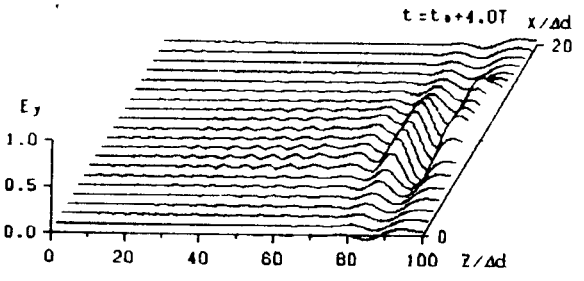

(d)

Fig 7 Time variation of pulse wave in microstrip line at $\theta = 45°$.

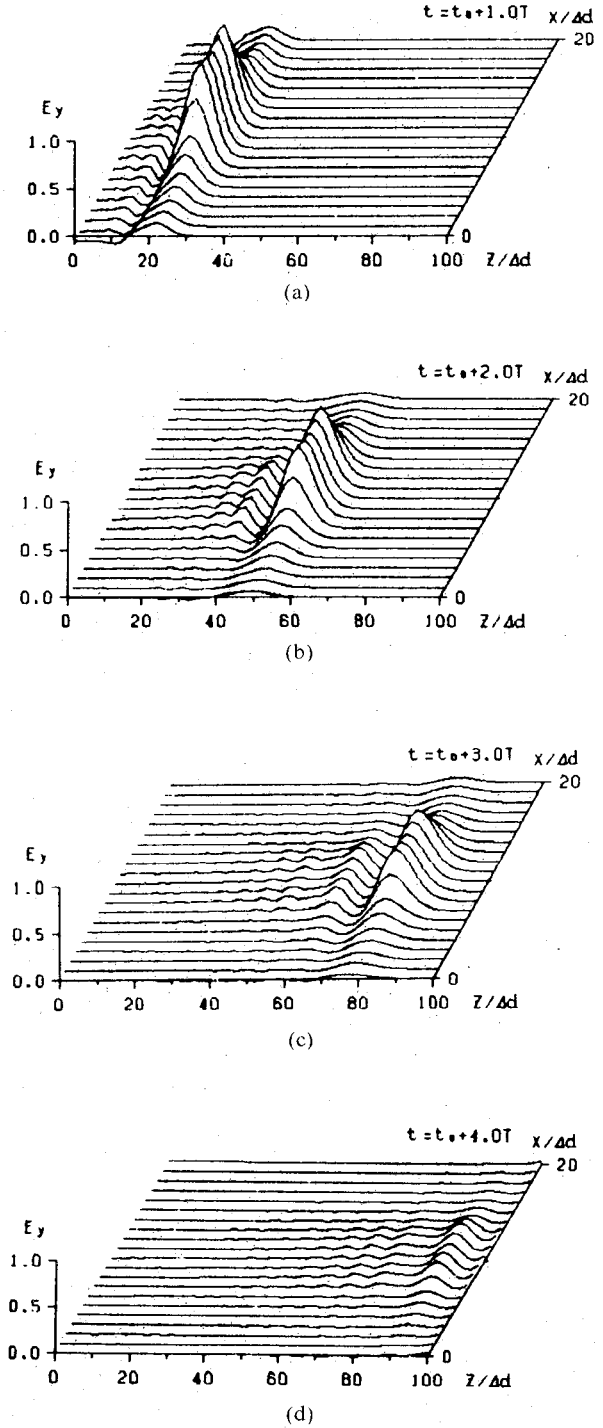

Fig. 8. Time variation of pulse wave in microstrip line at $\theta = 90°$.

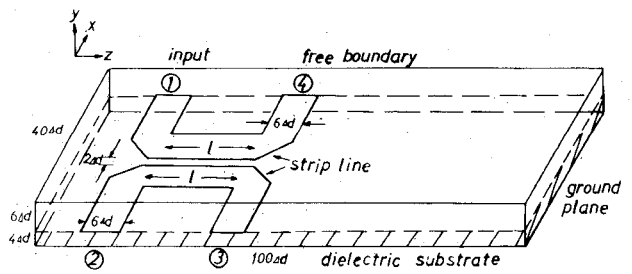

Fig. 9. Parallel-line-type directional coupler.

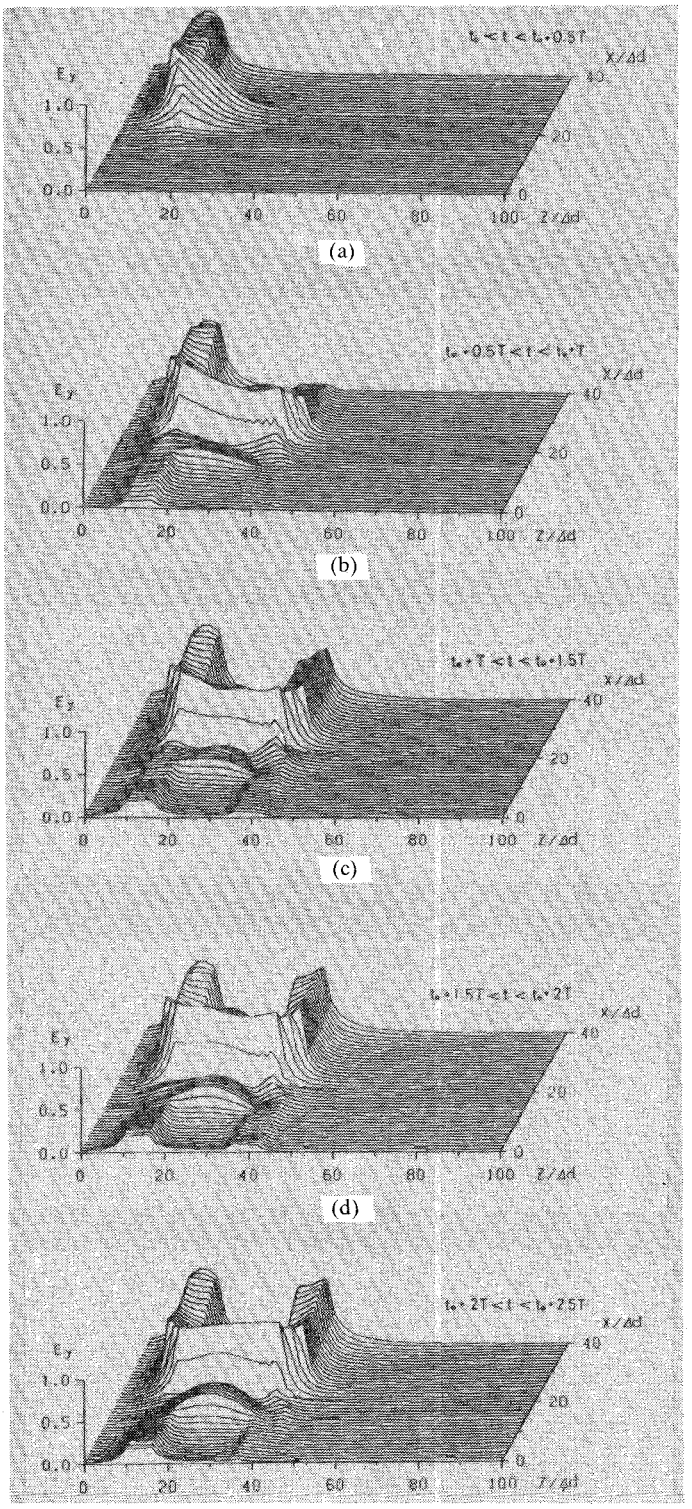

Fig. 10. Time variation of spatial distribution of electric field E_y in directional coupler at $\theta = 0°$.

propagation velocity of the pulse wave. The pulse shape is a positive half-period of a sinusoidal wave having $T = 71\,\Delta t$. Figs. 6–8 clearly show an increasing tendency of propagation velocity with increasing tilt angle, in agreement with the physical reasoning described in the previous section. The variable t_0 in the figures is an initial time at which the input wave is applied.

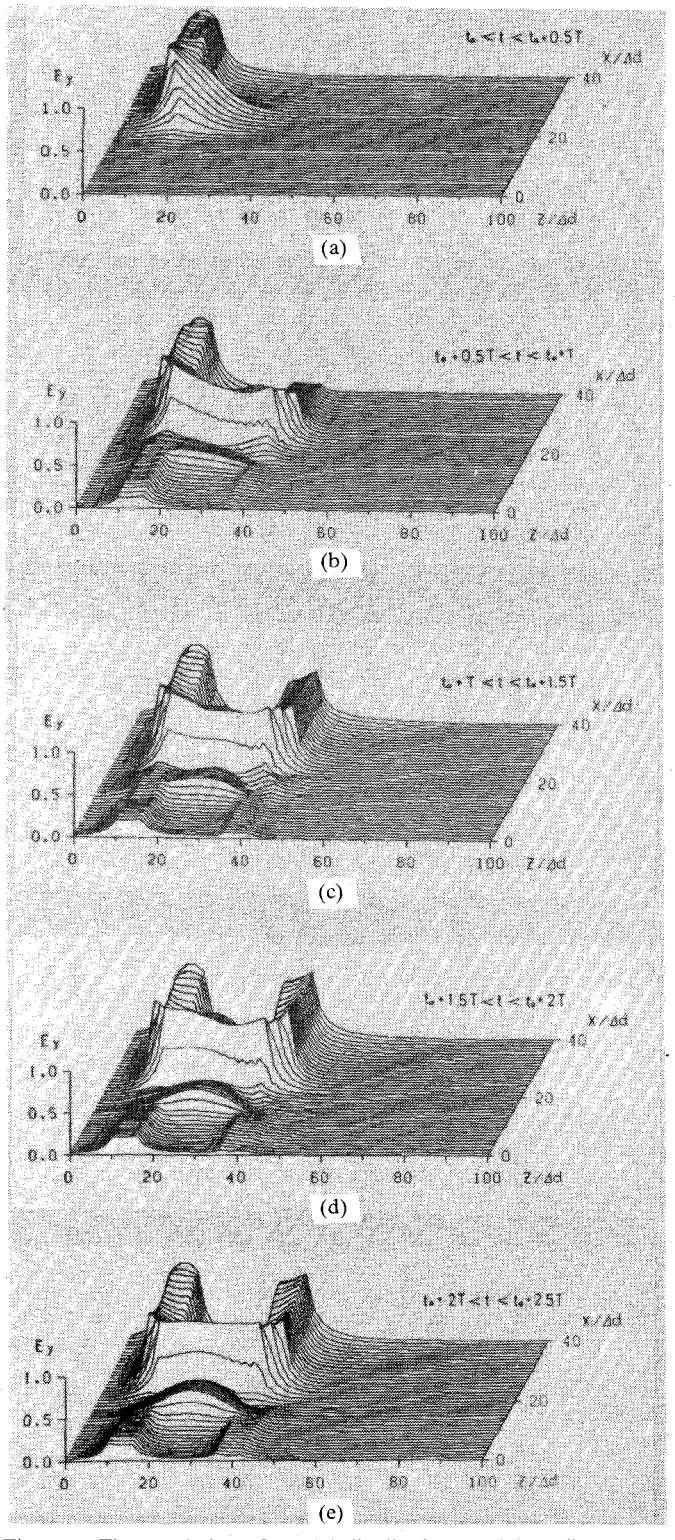

Fig. 11. Time variation of spatial distribution of electric field E_y in directional coupler at $\theta = 45°$.

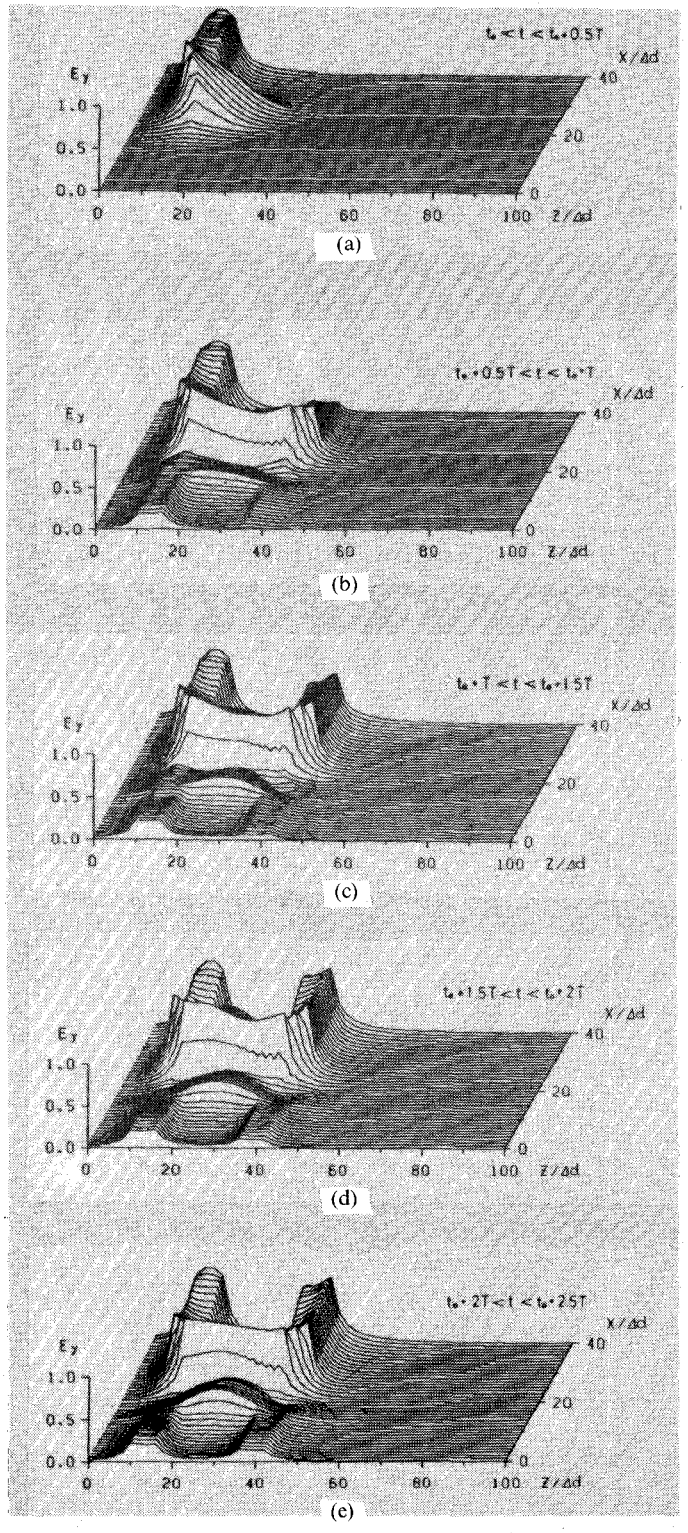

Fig. 12. Time variation of spatial distribution of electric field E_y in directional coupler at $\theta = 90°$.

C. Characteristics of the Directional Coupler

In order to show the effect of anisotropy on the coupling between the lines, a parallel-line-type directional coupler is analyzed and its characteristics are presented as a function of the tilt angle of the anisotropic axis. Fig. 9 shows the directional coupler. The dimensions in the x, y, and z directions of the analyzed region are 40, 10, and $100\Delta d$, respectively. The strip and ground conductor are assumed to have infinite conductivity. There is an anisotropic substrate with thickness $4\Delta d$ on the ground plane, and strip conductors with width $6\Delta d$ form the directional coupler. The upper region is an air layer with thickness $6\Delta d$. The upper and side boundary of the analyzed region is approximated by a free boundary condition. The fundamen-

tal property of the directional coupler taken in this analysis is that an input at port 1 gives an output at ports 2 and 4, and no output at port 3. The anisotropic substrate is assumed to be sapphire. The frequency of the input sinusoidal wave and the distance between ports 2 and 3 are adjusted to give maximum isolation for port 3 at $\theta = 0°$. The period of the input wave is $256\Delta t$ and "l" in Fig. 9 is $20\Delta d$. Figs. 10, 11, and 12 show the time variations of the spatial distribution, that is, the envelope of the maximum value at each point of the electric field E_y for $\theta = 0°$, 45°, and 90°, respectively. The expressions in the figures are the time intervals of a half-period used for finding the maximum value at each point to provide the spatial distribution rather than the instantaneous values. As the dimensions of each part of the coupler are very small compared with the guide wavelength, and the matching condition is realized at each port, the distributions seem to be from a pulse source. These figures look almost the same, but show the fine changes of the directional characteristics as a function of the tilt angle. Also, the time variation of each figure indicates the process by which the steady-state characteristics are obtained. The decrease of isolation is due to the decrease of ε_{eff} and the change of relative values between the Z_{0e} and Z_{0o}, as shown in Fig. 5. In this case, the CPU time is about 22 seconds for 700 iterations in the time domain using the HITACHI S-810/10 Super Computer at the Hokkaido University Computing Center.

IV. Conclusions

The fundamental formulation of an anisotropic medium using a permittivity tensor with off-diagonal terms is described for a three-dimensional transient analysis by Bergeron's method. The variation of the impedance and effective dielectric constant with the tilt angle θ is discussed to verify the validity of the formulation. Furthermore, to demonstrate the effect of anisotropy on the coupling property between lines, a parallel-stripline-type directional coupler is simulated.

In later work the treatment of tilting the anisotropic axis will be generalized. In addition to the directional coupler, other MIC devices will be analyzed and field variations will be simulated in the time domain to obtain the propagation characteristics of the high-speed pulse.

References

[1] B. Bhat and S. K. Koul, "New approach to strip- and microstrip-like transmission lines with anisotropic substrate having a tilted optical axis," *Proc. Inst. Elec. Eng.*, vol. 131, pt. H, no. 3, pp. 191–197, June 1984.

[2] M. Horno, "Upper and lower bounds on capacitances of coupled microstrip lines with anisotropic substrate," *Proc. Inst. Elec. Eng.*, vol. 129, pt. H, no. 3, pp. 89–93, June 1982.

[3] N. G. Alexopoulos and C. M. Krowne, "Characteristics of single and coupled microstrips on anisotropic substrates," *IEEE Trans. Microwave Theory Tech.*, vol. MTT-26, pp. 387–393, June 1978.

[4] M. Kobayashi and R. Terakado, "Method for equalizing phase velocities of coupled microstrip lines by using anisotropic substrate," *IEEE Trans. Microwave Theory Tech.*, vol. MTT-28, pp. 719–722, July 1980.

[5] T. Kitazawa and Y. Hayashi, "Coupled slots on an anisotropic sapphire substrate," *IEEE Trans. Microwave Theory Tech.*, vol. MTT-29, pp. 1035–1040, Oct. 1981.

[6] K. S. Yee, "Numerical solution of initial boundary value problems involving Maxwell's equations in isotropic media," *IEEE Trans. Antennas Propagat.*, vol. AP-14, no. 3, pp. 302–307, May 1966.

[7] A. Taflove and M. E. Brodwin, "Numerical solution of steady-state electromagnetic scattering problems using the time-dependent Maxwell's equations," *IEEE Trans. Microwave Theory Tech.*, vol. MTT-23, Aug. 1975.

[8] S. Akhtarzad and P. B. Johns, "Solution of Maxwell's equations and time by the t.l.m. method of numerical analysis," *Proc. Inst. Elec. Eng.* vol. 122, no. 12, pp. 1344–1348, Dec. 1975.

[9] S. Akhtarzad and P. B. Johns, "Three-dimensional transmission-line matrix computer analysis of microstrip resonators," *IEEE Trans. Microwave Theory Tech.*, vol. MTT-23, pp. 990–997, Dec. 1975.

[10] G. E. Mariki and C. Yeh, "Dynamic three-dimensional TLM analysis of microstrip lines on anisotropic substrate," *IEEE Trans. Microwave Theory Tech.*, vol. MTT-33, pp. 789–799, Sept. 1985.

[11] N. G. Alexopoulos, "Integrated-circuit structures on anisotropic substrates," *IEEE Trans. Microwave Theory Tech.*, vol. MTT-33, pp. 847–881, Oct. 1985.

[12] N. Yoshida and I. Fukai, "Transient analysis of a stripline having a corner in three-dimensional space," *IEEE Trans. Microwave Theory Tech.*, vol. MTT-32, pp. 491–498, May 1984.

[13] S. Koike, N. Yoshida, and I. Fukai, "Transient analysis of microstrip gap in three-dimensional space," *IEEE Trans. Microwave Theory Tech.*, vol. MTT-33, pp. 726–730, Aug. 1985.

[14] S. Koike, N. Yoshida, and I. Fukai, "Transient analysis of a directional coupler using a coupled microstrip slot line in three-dimensional space," *IEEE Trans. Microwave Theory Tech.*, vol. MTT-34, pp. 353–357, 1986.

[15] S. Koike, N. Yoshida, and I. Fukai, "Transient analysis of coupling between crossing-lines in three-dimensional space," *IEEE Trans. Microwave Theory Tech.*, vol. MTT-35, pp. 67–71, Jan. 1987.

[16] N. Yoshida, I. Fukai, and J. Fukuoka, "Application of Bergeron's method to anisotropic media," *Trans. IECE Japan*, vol. J64-B, pp. 1242–1249, Nov. 1981.

[17] N. Yoshida, I. Fukai, and J. Fukuoka, "Transient analysis of three-dimensional electromagnetic fields by nodal equations," *Trans. IECE Japan*, vol. J63-B, pp. 876–883, Sept. 1980.

Shoichi Koike (M'87) was born in Hokkaido, Japan, on February 21, 1959. He received the B.E. degree in electrical engineering from Yamanashi University, Kofu, Japan, in 1981, becoming a research student in the same university, and later receiving the M.E. and D.E. degrees in electrical engineering from Hokkaido University, Sapporo, Japan, in 1984 and 1987, respectively. He presently is engaged in the Space and Satellite Communication Systems Laboratory at the Space and Radio Division of Fujitsu Laboratories Ltd., Kawasaki.

Dr. Koike is a member of the Institute of Electronics, Information and Communication Engineers of Japan.

Norinobu Yoshida (M'87) was born in Hokkaido, Japan, on May 27, 1942. He received the B.E. and M.E. degrees in electronics engineering from Hokkaido University, Sapporo, Japan, in 1965 and 1967, respectively, and received the D.E. degree in electrical engineering there in 1982.

He joined the Nippon Electric Company, Ltd., Tokyo, in 1967, and was engaged in CAD at the Integrated Circuit Division. He became a Research Assistant in 1969 in the Department of Electrical Engineering in the Faculty of En-

gineering at Hokkaido University. He became a Lecturer in 1983, and an Associate Professor in 1984 in the same department. He is presently engaged in research in numerical methods for transient analysis of electromagnetic fields.

Dr. Yoshida is a member of the Institute of Electrical Engineers of Japan and the Institute of Electronics, Information and Communication Engineers in Japan.

✠

Ichiro Fukai (M'87) was born in Hokkaido, Japan, on August 21, 1930. He received the B.E., M.E., and D.E. degrees in electrical engineering from Hokkaido University, Sapporo, Japan, in 1953, 1956, and 1976, respectively.

In 1956, he joined the Defense Agency Technical Research and Development Institute. He became a Research Assistant in 1959 on the Faculty of Engineering at Hokkaido University and an Associate Professor at the Technical Teacher's Training Institute in 1961. In 1968 he became an Associate Professor and in 1977 a Professor in the Department of Electrical Engineering of the Faculty of Engineering at Hokkaido University.

Dr. Fukai is a member of the Institute of Electrical Engineers of Japan and the Institute of Electronics, Information and Communication Engineers in Japan.